Available online at www.sciencedirect.com
ScienceDirect

NUCLEAR SCIENCE AND TECHNIQUES

Nuclear Science and Techniques 19 (2008) 266-273

Field evolution of harmonic radiation in an HGHG FEL

DENG Haixiao[1,2] LI Dongguo[1] DAI Zhimin[1,*]

[1] Shanghai Institute of Applied Physics, Chinese Academy of Sciences, Shanghai 201800, China

[2] Graduate University of the Chinese Academy of Sciences, Beijing100049, China

Abstract As a natural character of high gain free electron laser (FEL), harmonic radiation is regarded as the natural extensions to short wavelengths. In high gain harmonic generation (HGHG) scheme, harmonic evolution may be attributed to the initial harmonic bunching, self amplification of the harmonic radiation, electron beam strongly bunched by the fundamental radiation, the faster longitudinal dynamics and the fundamental synchrotron oscillation. It is more complex than harmonic evolution in other FEL schemes. In this paper, via theoretical analyses and three dimensional simulations, a general description of different aspects of harmonic evolution in the HGHG process is presented.

Key words Harmonic, FEL, HGHG, Nonlinearity

CLC number TN248.6

1 Introduction

Currently, at the end of a free electron laser (FEL) undulator, most self amplified spontaneous emission (SASE)[1] and high gain harmonic generation (HGHG)[2,3] are in deep saturation regime[4,5]. One of the natural characters of such high gain FEL is harmonic radiation which has been theoretically analyzed[6-8] and numerically investigated[9,10]. It shows that significant powers of the first few harmonic radiations are generated in high gain FEL. In more details, the output power of the 3rd harmonic radiation is about 1% of the fundamental level[7], which is about 8 orders of magnitude brighter than a top rank synchrotron radiation light source[11]. These theoretical predictions have been realized in the first harmonic measurement at VISA FEL[12]. Thus, harmonic radiation is a significant extension to short wavelengths, and of great interests.

In HGHG, the fundamental frequency conversion is based on the ratio of resonant frequencies of the modulator and radiator. The harmonic radiations in a radiator are high harmonics of the seed laser. This means that the bunching corresponding to the high harmonics could be rich and significant. Such a character makes harmonic radiations in HGHG FEL even more fruitful and attainable than those found in SASE. Also, it makes harmonic evolution much more complex than in other FEL scheme. However, the early work of harmonic radiation in HGHG FEL mainly refers to the nonlinear harmonic generation, which is driven by the fundamental and grows faster than the fundamental.

In this paper, the harmonic evolution in HGHG FEL is discussed. A theoretical discussion of harmonic evolution is presented in Section 2. The validation of theoretical analyses and the harmonic performance obtained by three dimensional (3D) simulations are given in Section 3. The conclusions are in Section 4.

Partially supported by the Key Project for Promoting Fundamental Research in China (Grant No. 2002CB713600)

* Corresponding author. *E-mail address:* daizhimin@sinap.ac.cn

Received date: 2008-07-09

2 Mechanism of harmonic evolution in HGHG

As a relativistic electron beam with average energy $\gamma_0 mc^2$ entering a planar radiator in the z direction, one observes the transverse wiggling motion together with the "figure of eight" longitudinal phase oscillations in the resonant frame. This trajectory generates harmonic radiation. We denote the fundamental wavelength by λ_s and the period length of the radiator magnet by λ_w. The corresponding wave numbers are $k_s= 2\pi/\lambda_s$ and $k_w= 2\pi/\lambda_w$. Then, we introduce the famous dimensionless variables

$$\begin{aligned} &\tau = k_w z \\ &x = r\sqrt{2k_s k_w} \\ &p = \mathrm{d}x/\mathrm{d}\tau \\ &k = k_\beta / k_w \\ &f = \sum_{n=0}^{¥} F_n e^{in\theta} + c.c. \end{aligned}$$

where $\theta=k_wz+k_sz-\omega_st+\xi\sin(2k_wz)$ describes the FEL bunching, $r = (x, y)$ is the transverse coordinates, $k_\beta = 2\pi/\lambda_\beta$ is the wave numbers of transverse oscillation, n is the odd number, F_0 represents the initial smooth distribution in the absence of the radiation field, and other components F_n, near $e^{in\theta}$, means corresponding electron beam bunching that contribute to the growth of the n-th harmonic. Therefore, the coupled Maxwell-Vlasov equations may be written as

$$(\frac{\partial}{\partial\tau}+\frac{\partial}{\partial\theta}-\frac{i}{n}\nabla_\perp^2]E_n = \frac{D_{1n}}{\gamma_0}\int \mathrm{d}\gamma\int F_n \mathrm{d}^2 p \quad (1)$$

$$\begin{aligned}&(\frac{\partial}{\partial\tau}+\theta'\frac{\partial}{\partial\theta}+p\frac{\partial}{\partial x}-k^2x\frac{\partial}{\partial p})(\sum_{n=0}^{\infty}F_n e^{in\theta}) = \\ &(\sum_{n=1}^{\infty}\frac{D_{2n}}{\gamma}E_n e^{in\theta})\frac{\partial}{\partial\gamma}(\sum_{n=0}^{\infty}F_n e^{in\theta}) \end{aligned}\quad (2)$$

with $D_{1n} = n_0\mu_0 ec^2K[JJ]_n/2k_w$, $D_{2n} = eK[JJ]_n/4k_wmc^2$, and

$$\begin{aligned}&\theta' = 2\frac{\gamma-\gamma_0}{\gamma_0}-\frac{1}{4}(p^2+k^2x^2) \\ &\gamma' = \sum_{n=1}^{\infty}\frac{D_{2n}}{\gamma}\times E_n e^{in\theta}+c.c.\end{aligned}\quad (3)$$

where K is the dimensionless undulator parameter, E_n is the complex slowly varying envelope function of the n-th harmonic, $\nabla_\perp^2$ is the transverse Laplacian, μ_0 is the permeability of free space and $[JJ]_n$ is the difference of the Bessel functions defined as

$$[JJ]_n=(-1)^{(n-1)/2}[J_{(n-1)/2}(n\xi)-J_{(n+1)/2}(n\xi)]$$

where $\xi=K^2/(4+2K^2)$.

According to Eq.(1), the n-th harmonic is determined by the term F_n. Thus, we separate the different order of $e^{i\theta}$ in Eq.(2) and introduce Fourier transform over θ and Laplacian transform over τ. Then, the Maxwell-Vlasov equations can be reduced to[13]

$$(-i\Omega+iq-\frac{i}{n}\nabla_\perp^2]\overline{E}_n = \frac{D_{1n}}{\gamma_0}\int\mathrm{d}\gamma\int\overline{F}_n\mathrm{d}^2p \quad (4)$$

$$\begin{aligned}&[-i\Omega+i\theta'(q+n)+p\frac{\partial}{\partial x}-k^2x\frac{\partial}{\partial p}]\overline{F}_n = \\ &\sum_{v=0}^{u+v=n}\frac{D_{2u}}{\gamma_0}\overline{E}_u\frac{\partial\overline{F}_v}{\partial\gamma}\end{aligned}\quad (5)$$

where $\overline{E}_n$ and $\overline{F}_n$ are the transformed functions of E_n and F_n. Since we deal with FEL eigenvalue problems, the initial value processes were neglected in Eqs.(4) and (5).

2.1 Coherent harmonic generation

In the modulator of HGHG, the seed laser and the electron beam interact with each other to modulate the electron beam energy. Then, the energy modulation is converted into spatial modulation *via* passing through the dispersive section. Since the harmonic radiation in the radiator is high harmonic of the seed laser, the electron beam may enter the radiator with a significant harmonic bunching parameter. It can be evaluated by Eq.(6)[14]

$$\begin{aligned}&|b_n| \equiv |\langle e^{-in\theta_j}\rangle| = |\int\mathrm{d}\gamma\int F_n\mathrm{d}^2p| = \\ &e^{-\frac{1}{2}(nm\frac{\partial\theta}{\partial\gamma}\sigma_\gamma)^2}J_{nm}[nm\frac{\partial\theta}{\partial\gamma}\Delta\gamma]\end{aligned}\quad (6)$$

where b_n is bunching factor of the n-th harmonic, <> represents an average over the beam, m is the frequency up-conversion number of HGHG, σ_γ is the initial energy spread of the electron bunch, Δ_γ is the maximum energy modulation at the end of the modulator, and $\partial\theta/\partial\gamma$ is the strength of the dispersive section.

At the beginning of the radiator, the radiated field is so weak that it does not change the electron distribution much in short distance, and this process can be approximated as many rigid microbunching[2]. Thus, Eqs.(2) and (3) can be neglected, and one dimensional (1D) case of Eq.(1) is given as

$$\frac{\partial\theta}{\partial\tau}E_n=\frac{D_{1n}}{\gamma_0}b_n \tag{7}$$

Therefore, the harmonic field grows linearly with z, and the harmonic power grows quadratically. Such a kind of radiation is called coherent harmonic generation (CHG). After about two gain lengths, the longitudinal dynamic of the electron beam induced by the radiated fields become important, then we must consider the Eqs.(3), (4) and (5) together.

2.2 Linear harmonic generation

In general, the solutions for the harmonic bunching and field amplitude are combinations of two different components, one given by the decoupled linear analysis, and the other driven by the exponential instability of the lower nonlinear harmonics and the fundamental radiation[4]. In Eq.(5), the term v=0 represents linear harmonic generation (LHG), which is caused by the self amplification of the harmonic radiation, and other terms represent nonlinear harmonic generation (NHG) due to strongly bunched electron beams. Simply one can deal the two components separately.

Assuming a uniform longitudinal density, a uniform "water-bag" transverse density $u(p^2+k^2x^2)$ and a Gaussian distribution $h(\gamma)$ around the value of γ_0 with *rms* energy spread σ_γ, a dispersive relation determining the complex growth rate μ_n and the transverse mode profile $\overline{E}_n$ is derived

$$\begin{aligned}(\mu_n+\frac{1}{n}\nabla_\perp^2)\overline{E}_n=D_{1n}D_{2n}\int\frac{h'(\gamma)}{\gamma^2}\mathrm{d}\gamma\times\\ \int\mathrm{d}^2pu(p^2+k^2x^2)\times\\ \int\mathrm{d}s\mathrm{e}^{-\mathrm{i}\alpha_n s}\overline{E}_n[x\cos ks+(p/k)\sin ks]\end{aligned} \tag{8}$$

where $\alpha_n=\mu_n+(\omega-\omega_r)/\omega_r-n\theta'$. According to FEL process, a Gaussian test function is introduced to solve Eq.(8) by variational approximation method[15]. Then, the 3D gain function of linear harmonic generation can be expressed in the scaled form

$$\frac{\mathrm{Im}(\mu_n)}{D_n}=G(k_s\varepsilon,\frac{\sigma_\gamma}{D_n},\frac{k}{D_n},\frac{\omega-\omega_s}{\omega_s D_n}) \tag{9}$$

The scaling parameter D_n is a measure of transverse electron current. The intrinsic property of the variational approximation method assures that the error of the eigenvalue μ_n depends quadratically on the small errors in the test function. Moreover, for the electron beam with Gaussian transverse density, results may be found in Ref.[7].

2.3 Nonlinear harmonic generation

NHG occurs when the electron beam is strongly bunched in the ponderomotive potential formed by the undulator field and the radiation field of the fundamental frequency. To determine nonlinear harmonic interactions, we consider only the nonlinear components and neglect the linear component in Eq.(5), which can be rewritten as

$$\begin{aligned}[-\mathrm{i}\Omega+\mathrm{i}\theta'(q+n)+p\frac{\partial}{\partial \mathrm{x}}-k^2x\frac{\partial}{\partial p}]\overline{F}_\mathrm{n}=\\ \sum_{v=1}^{u+v=n}\frac{D_{2u}}{\gamma_0}\overline{E}_u\frac{\partial\overline{F}_v}{\partial\gamma}\end{aligned} \tag{10}$$

The even harmonic on the right side of Eq.(10) may be neglected in planar radiator. And the main contribution to NHG is from the fundamental radiation. Then, the 1D dispersive relation for the 3rd NHG is given by

$$\overline{E}_3\propto D_{13}{D_{21}}^3{\overline{E}_1}^3 \tag{11}$$

For the 5th NHG, the leading nonlinear terms are

$$\overline{E}_5\propto D_{15}({D_{21}}^5{\overline{E}_1}^5+{D_{21}}^2{\overline{E}_1}^2D_{23}\overline{E}_3) \tag{12}$$

From these relations, we can conclude that NHG grows faster than the fundamental radiation, and the gain length scales inversely with the harmonic order. NHG offer significant power in the short-wavelength, therefore extending the applications of FEL scheme.

2.4 Saturation of harmonic generation

E_n and b_n can be writen as $|E_n|\exp(i\varphi_n)$ and $|b_n|\exp(i\psi_n)$. Thus, 1D form of Eq.(1) can be reduced to

$$\frac{\partial}{\partial\tau}|E_n|+i|E_n|\frac{\partial}{\partial\tau}\phi_n=\frac{D_{1n}}{\gamma_0}|b_n|\mathrm{e}^{\mathrm{i}(\psi_n-\phi_n)} \quad (13)$$

According to Eq.(13), the FEL gain of the n-th harmonic is determined by the difference of the angle of the n-th harmonic radiation field and the n-th harmonic bunching. A variable $\varDelta_n$ with the variation region [–π, π] is defined as

$$\varDelta_n=\psi_n-\phi_n \quad (14)$$

Therefore, once $\varDelta_n$ lies in [-0.5π, 0.5π], radiation power of the n-th harmonic grows, and for other cases, radiation power of the n-th harmonic decreases.

Comparing with the fundamental radiation, the radiation field of the harmonic is small and could be neglected in Eq.(3). The bunching process of the electron beam is mainly driven by the fundamental. In such a system, the growth rates of the two terms on the right side of Eq.(14) are n times of the ones in the fundamental[6]. Thus a rough estimate can be concluded

$$\frac{\partial}{\partial\tau}\varDelta_n\cong n\frac{\partial}{\partial\tau}\varDelta_1 \quad (15)$$

For the FEL process of the fundamental radiation, at the beginning of the radiator, $\varDelta_1$ would be around zero and the radiation grows exponentially. As the radiation grows, $\varDelta_1$ slips out [−0.5π, 0.5π] and runs into [–π, –0.5π] or [0.5π, π], hence the saturation followed by decreased fundamental radiation. This is known as FEL synchrotron oscillation.

For the case of the harmonic radiation, $\varDelta_n$ varies n times faster than the fundamental and runs into the decrease region earlier than the fundamental. Therefore, a saturation of harmonic generation (SHG) is expected to appear earlier than the fundamental radiation. And the higher the harmonic order is, the earlier it saturates [8]. The saturation power of the n-th harmonic radiation can be estimated by inserting $\varDelta_n$=π/2 into Eq.(13). A typical saturation power of the 3rd and the 5th harmonic radiation should be 0.85% and 0.02% of the fundamental, respectively.

2.5 Regain of harmonic generation

Regain of harmonic generation (RHG) is observed in 1D simulations[6] and 3D simulations[9,10] of harmonic radiation. However, no special attention was paid on it. As shown in Fig.1, when NHG becomes dominant after 25m long radiator, $\varDelta_3$ changes faster and arrives –0.5π earlier than $\varDelta_1$, hence the SHG occurs at point A, where $\varDelta_1$ is only about –0.27π. While the fundamental radiation saturates at $\varDelta_1$ = –0.5π, $\varDelta_3$ has oscillated one period and become –0.12π (point B). Finally, while $\varDelta_3$ reaches –0.5π again, RHG comes out (point C). Generally, in RHG process, the 3rd harmonic radiation power can be doubled.

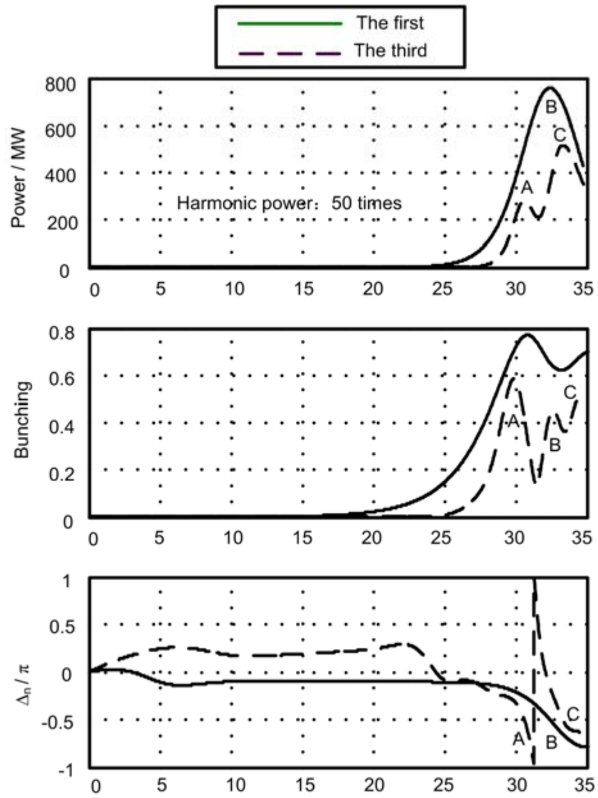

Fig.1 Performances of the fundamental and the 3rd harmonic radiation solved from one dimensional FEL equations.

The RHG progress can be better understood by analyzing the FEL longitudinal dynamics. Despite a similar qualitative tendency, the bunching factor of the 3rd harmonic shown in Fig.1 has a smaller modulus. The peak has a shorter length along the radiator axis. The narrower length with respect to the fundamental radiation is due to the faster longitudinal dynamic.

One adjunctive result by the dynamic is the fact that when Δ_3 runs out of [$-\pi/2$, $\pi/2$], and enters the decrease area of the 3rd harmonic radiation power, the bunching factor of the 3rd harmonic radiation lies in a valley. In contrary, when Δ_3 runs into [$-\pi/2$, $\pi/2$] again, the bunching factor of the 3rd harmonic just lies on its second peak. The difference in the harmonic radiation oscillation contributes to regain and doubling of the 3rd harmonic radiation power after its first saturation.

3 Simulation performance

In this section, we numerically investigate the field evolution process of the harmonic radiation in HGHG FELs, with parameters (Table 1) proposed for the Shanghai Soft X-ray FEL scheme (SXFEL)[16]. The steady-state simulations up to the 3rd harmonic are performed by Genesis2.0[17]. Fig.2 shows the power growth of the fundamental 9 nm radiation and the 3rd harmonic 3 nm radiation as a function of the radiator length for SXFEL, where the region of CHG, LHG, NHG, SHG and RHG can be well recognized. Applying the theoretical analyses in Section 2, one obtains the simulation results.

Table 1 Main parameters of 9-nm HGHG in SXFEL

Parameters	Values
Electron beam energy E / GeV	0.84
Peak current I_P / A	600
Normalized emittance ε / mm-mrad	2
Local energy spread σ_γ/γ	1×10^{-4}
Seed laser wavelength λ_S / nm	45
Seed laser power P_S / MW	0~50
Modulator period length λ_{UM} / cm	3.8
Modulator length L_M / m	1
Modulator undulator parameter K_M	3.22
Dispersive strength $\partial\theta/\partial\gamma$	0~15
Resonant wavelength λ_R / nm	9
Radiator period length λ_{UR} / cm	2.5
Radiator undulator parameter K_R	1.41

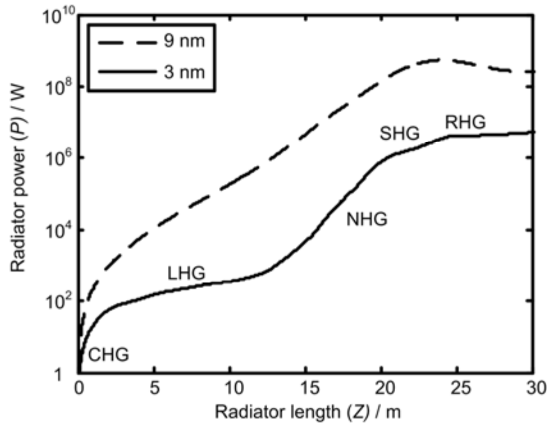

Fig.2 CHG-LHG-NHG-SHG-RHG (CLNSR) process of the 3rd harmonic radiation in 9-nm SXFEL. P_s=0.1 MW, $\partial\theta/\partial\gamma$=9.2.

1) Due to the initial harmonic bunching, CHG with about 100 W is generated at the 3rd harmonic radiation in the first 2~3 m of the radiator, which is about 0.2% of the fundamental CHG level. From a rough estimation, $|b_3|$ is approximately $0.1|b_1|$ at the entrance of the radiator.

2) The following 10 m of the radiator is LHG caused by self amplification of the 3rd harmonic radiation. The gain length of the 3rd LHG is much more slowly than the fundamental radiation. This is due to lower coupling coefficient and more sensitive to the energy spread, peak current and emittance of electron beam than that of the fundamental radiation. The simulated gain length of the 3rd LHG is 4.66 m, which agrees with the analytical gain length of 4.43 m from Eq.(9).

3) The electron beam covering 13 m of the radiator, where the power of 9 nm radiation reaches 1 MW, is strongly bunched by the fundamental radiation, and NHG occurs. Passing 6 meters more in the radiator, the electrons lead to the 3rd harmonic radiation power growth of 1 MW from 1 kW.

4) When the fundamental radiation power achieves 242 MW at 21 m, SHG of the 3rd harmonic 3 nm radiation occurs with saturation power of 1.3 MW, which is earlier than the fundamental saturation.

5) Together with synchrotron oscillation followed by the fundamental saturation with power of 557 MW, RHG makes the 3rd harmonic radiation power achieve 4.2 MW.

In Fig.2, CHG, LHG, NHG, SHG and RHG dominate in different positions of the radiator, and can be clearly recognized. However, all the five mechanisms of harmonic evolution coexist under very strict conditions. More generally in harmonic evolution, different mechanisms compete with each other, and this leads to different processes of harmonic evolution. The five most potential processes of harmonic evolution in HGHG, which are defined as CLNSR, NSR, LNSR, CSR and CNSR, respectively, are shown in Figs.2~6.

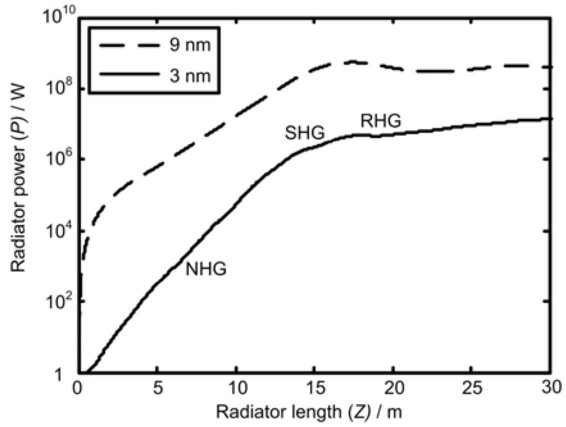

Fig.3 NHG-SHG-RHG (NSR) process of the 3rd harmonic radiation in 9-nm SXFEL. P_s=5 MW, $\partial\theta/\partial\gamma$= 1.0.

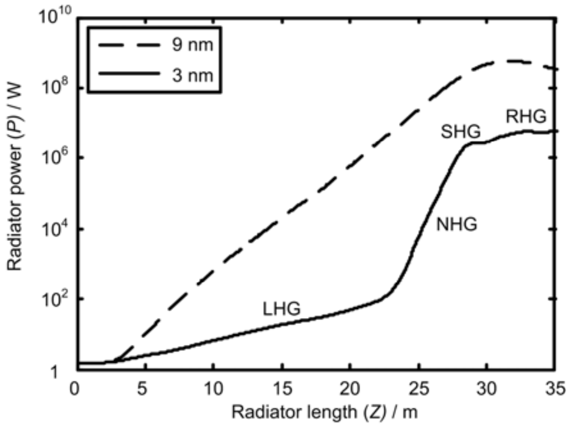

Fig.4 LHG-NHG-SHG-RHG (LNSR) process of the 3rd harmonic radiation in 9-nm SXFEL. P_s=2 MW, $\partial\theta/\partial\gamma$=0.

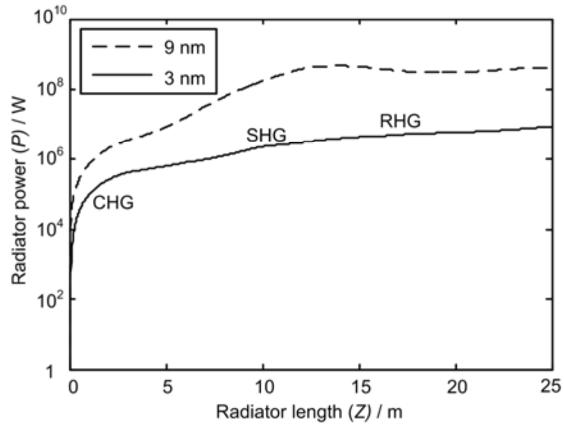

Fig.5 CHG-SHG-RHG (CSR) process of the 3rd harmonic radiation in 9 nm SXFEL. P_s=10 MW, $\partial\theta/\partial\gamma$=2.0.

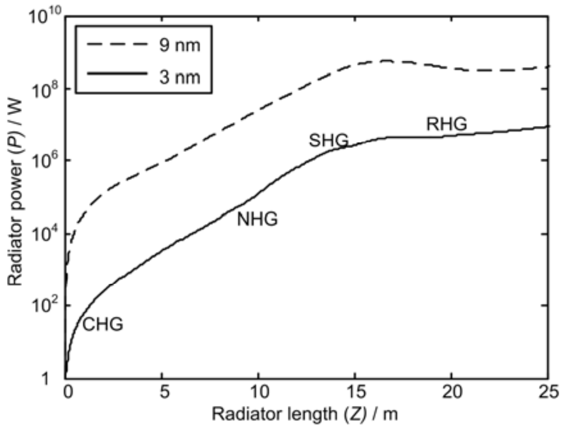

Fig.6 CHG-NHG-SHG-RHG (CNSR) process of the 3rd harmonic radiation in 9-nm SXFEL. P_s=3 MW, $\partial\theta/\partial\gamma$=1.6.

Harmonic evolution in HGHG is much related to quality of the beam entering a radiator, especially the bunching and energy spread. The bunching is determined by *rms* energy spread induced by the seed laser and the strength $\partial\theta/\partial\gamma$ of the dispersive section.

Next, by a scan simulation through the practical range of the FEL parameters, we illuminate the appearance condition of different harmonic evolution processes of SXFEL 9 nm HGHG in Fig.7. Note that if the gain reduction as the beam energy spread increases to Landau damping, in the laboratory frame, significant harmonic radiation will occur when $\Delta_\gamma/\gamma < \rho_n = (2D_{1n}D_{2n})^{1/3}/2\gamma_0$. Thus, a practical limit $\Delta_\gamma/\gamma < \rho_n$ is employed in the scan simulation.

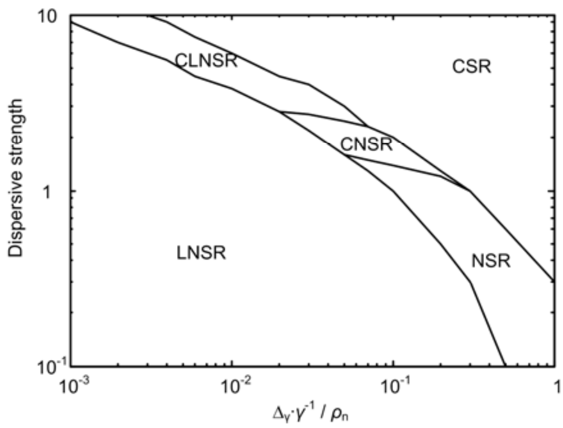

Fig.7 Simulated "five-region" that represent the condition of five harmonic evolution process in 9-nm SXFEL.

From Fig.7, the 3rd harmonic 3 nm experiences LNSR and CSR process for most cases. LNSR means limited spatial bunching induced by the modulator and the dispersive section, and the radiation starts from noise in the radiator, which works just as in SASE FEL. In LNSR process, LHG and NHG can be well recognized and their gain length can be well calculated. The gain length of the 3rd LHG and NHG of SXFEL is prettily consistent with analytical estimates. In contrary, CSR is the harmonic evolution in normal HGHG status, as suggested by Yu L H[18], who found intense seed signal induced in the modulator and strong coherent harmonic radiation generated in the radiator.

4 Concluding remarks

Harmonic radiation may extend the application of FEL facility to short-wavelength. Moreover, some FEL schemes aimed at enhancing the efficiency of harmonic radiation have been proposed[19,20]. Understanding of harmonic radiation is of great interest. In this paper, we present a general description of harmonic evolution in HGHG FEL. On the basis of 9 nm HGHG of SXFEL, different mechanisms in harmonic evolution are given. It was found that harmonic evolution might experience CHG, LHG, NHG, SHG and RHG, depending on initial harmonic bunching and energy spread of the electron beam entering the radiator. The numerical simulation results agree well with the theoretical analysis. This is useful in understanding harmonic evolution and stimulating discussions on future investigations.

Due to different beam qualities in the radiator, there can be five harmonic evolution processes in HGHG. Since the electron bunch enters the radiator with large energy spread, the harmonic power in HGHG operation at fundamental saturation is less than that in SASE operation, being respectively 4.2 MW and 5.6 MW in SXFEL. However, the required length of HGHG undulator is much shorter than that of SASE. Under such a circumstance, saturation condition of the 3rd harmonic radiation can only be satisfied in CSR process. In SXFEL case, a 15 m radiator is reasonable for fundamental saturation. Thus, the output power of the 3rd harmonic radiation in HGHG operation is 4.4 MW, with respect to 0.02 kW in SASE operation. A 100-fs seed laser will be injected in SXFEL because of the multi-stage HGHG principle. Once the radiations in the radiator saturate, they enter the superradiant regime. Then, the energy exchange between the electron beam and the harmonic field is proportional to the slippage length scaled with the fundamental resonant wavelength. One may find that the quadratic growth of the 3rd harmonic works until the SASE contribution stops the evolution of superradiant by ultimately spoiling the longitudinal phase space of the electrons[21].

Longitudinal dynamics of the electrons contributes to the harmonic radiation. It is prettily complicated and would be affected by many factors, such as the beam energies spread fluctuation due to the fundamental FEL synchrotron oscillation, the different optimal electron beam energy for the fundamental and for the harmonic radiation, the slower and the fast dynamics induced by LHG and NHG, respectively. An interesting phenomenon, the radiation power transfer from the fundamental to the harmonic radiation, may be expected. This, together with the slippage effects, however, will be a subject of a much more explicit study in future.

References

1 Pellegrini C. Nucl Instrum Methods Phys Res A, 1988, **272:** 364-367.

2 Yu L H. Phys Rev A, 1991, **44:** 5178-5193.

3 Yu L H, Babzien M, Ben-Zvi I, *et al*. Nucl Instrum Methods Phys Res A, 2000, **445**: 301-306.

4 Reiche S, Pellegrini C, Rosenzweig J, *et al*. Nucl Instrum Methods Phys Res A, 2002, **483:** 70-74.

5 Jaeschke E, *et al.* Nucl Instrum Methods Phys Res A, 2005, **543:** 85-89.

6 Bonifacio R, Salvo L De, Pierini P. Nucl Instrum Methods Phys Res A, 1990, **293:** 627-629.

7 Huang Z, Kim K J. Phys Rev E, 2000, **62:** 7295-7308.

8 Jia Q K. IEEE J Quantum Electron, 2007, **43**: 833-837.

9 Freund H P, Biedron S G, Milton S V. Nucl Instrum Methods Phys Res A, 2000, **445:** 53-58.

10 Biedron S G, Huang Z, Kim K J, *et al*. Nucl Instrum Methods Phys Res A, 2002, **483:** 101-106.

11 Tremaine A, Wang X J, Babzien M, *et al*. Phys Rev Lett, 2002, **88:** 204801.

12 Tremaine A, Wang X J, Babzien M, *et al*. Nucl Instrum Methods Phys Res A, 2003, **507:** 445-449.

13 Deng H X, Dai Z M. Chin Phys C, 2008, **32:** 297-302.

14 Bonifacio R, De Salvo L, Pierini P, *et al*. Nucl Instrum Methods Phys Res A, 1990, **296:** 787-790.

15 Xie M, Deacon D, Nucl Instrum Methods Phys Res A, 1986, **250:** 426-431.

16 Kong X C, Wang J Q, Wang S H, *et al*. Shanghai soft X-ray FEL test facility conceptual design report, 2008, Shanghai, Chapter 2: 1-20.

17 Reiche S. Proceeding of PAC07, Albuquerque, New Mexico, USA, 2007, 1269-1271.

18 Yu L H, Wu J H. Nucl Instrum Methods Phys Res A, 2002, **483**: 493-498.

19 Latham P E, Levush B, Antonsen T M, *et al*. Phys Rev Lett, 1991, **66**: 1442-1445.

20 Deng H X, Dai Z M. Nucl Sci Tech, 2008, **19**: 7-12.

21 Giannessi L, Musumeci P. New J Phys, 2006, **8**: 294.